Focal properties of the two-tube electrostatic lens for large and near-unity voltage ratios

D. DiChio* and S. V. Natali*

University of Bari, Bari, Italy

C. E. Kuyatt

National Bureau of Standards, Washington, D.C. 20234

(Received 26 November 1973)

Accurate calculations of focal properties of the two-tube electrostatic lens are extended to cover a range of voltage ratios from 1.1 to 10000. The accuracy of the calculations is discussed in detail. For voltage ratios near 6400 the lens is found to be telescopic. Results are given in tabular form and as $P-Q$ (object–image) curves. A simple analytical form for the focal properties of lenses with near-unity voltage ratios is given.

INTRODUCTION

Accurate values of the first-order focal properties of the two-tube electrostatic lens for voltage ratios between 1.5 and 50 are now available.[1,2] Recently[3,4] these calculations have been extended to higher voltage ratios. Such strong lenses are of interest in several areas; for example, for the deceleration of high energy beams to low energy for energy analysis, for the analysis of retarding potential analyzers, and for the analysis of lenses used to accelerate very low energy electrons produced in near-threshold processes. We have therefore extended these calculations to a voltage ratio of 10 000.

It is also useful to have data on weak lenses with voltage ratios near unity. Such lenses can be used to make small corrections to a strong lens, and also occur for certain operating conditions of the three-tube lens.[5,6] In the computer optimization of lens systems[7] one occasionally encounters voltage ratios near unity and these must be provided for in the computer program. A first approach to the representation of accurate focal properties for computer use was made by Galejs and Kuyatt.[8] Cubic splines were used, and it was found that the region near unity voltage had to be treated separately. We present here first-order focal properties for voltage ratios between 1.1 and 1.7.

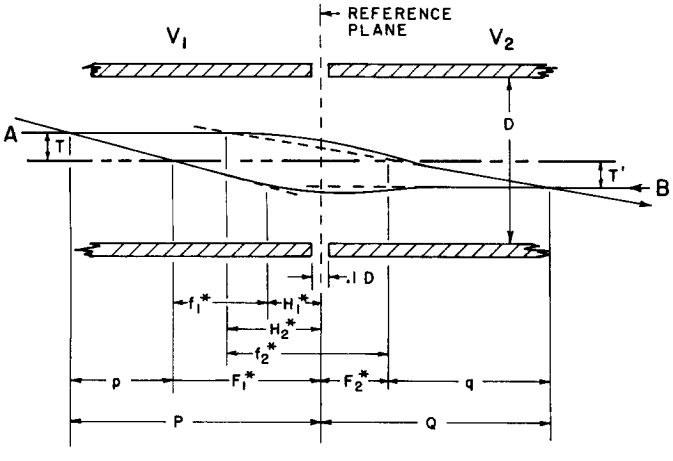

FIG. 1. Schematic drawing of the two-tube electrostatic lens showing the definition of the apparent focal points F_1^*, F_2^*, principal planes H_1^*, H_2^* and focal lengths f_1^*, f_2^*. The object and image coordinates are (p,P) and (q,Q), respectively.

SIGN CONVENTION

In our previous work[2,3,8–10] we have used a sign convention in which the focal lengths f_1, f_2, focal points F_1, F_2, and principal plane positions H_1, H_2 are all positive. These quantities are shown in Fig. 1, where the stars indicate that for finite distances T, T' of the rays from the axis of the lens the quantities shown differ from the first-order quantities and must be extrapolated to T, $T'=0$. This sign convention has served well for lenses which are not too strong. However, over the range extending to a voltage ratio of 10 000 there are several reversals in sign of the first-order focal properties. We therefore believe that a different sign convention[11,12] must be adopted in which the quantities F_1, F_2, H_1, and H_2 are negative if to the left of the reference plane and positive if to the right. It remains to choose a sign convention for f_1 and f_2. We have rejected the obvious choice of f_1 and f_2 positive for weak lenses in favor of having f_1 negative and f_2 positive, since this gives a simplification of some of the lens equations. For example, the form of the Newtonian lens equation

$$pq=f_1f_2 \tag{1}$$

is preserved, where p and q are the position of the object and image, respectively, from the first and second focal points, where these quantities are again negative if to the left of the corresponding focal point and positive if to the right. A symmetry is also obtained in the equations relating the focal points, principal planes, and focal lengths,

$$\begin{aligned} H_1&=F_1-f_1 \\ H_2&=F_2-f_2 \end{aligned} \tag{2}$$

so that one can be obtained from the other by interchanging the indices 1 and 2. This is an advantage in computer cal-

culations since one does not need different formulas for the left and right sides of a lens as would be necessary with other sign conventions. Finally, the quantities P and Q, the distances of the object and image, respectively, with respect to the reference plane are negative if to the left and positive if to the right. There is thus a complete uniformity in the sign convention for all quantities.

TESTS OF ACCURACY OF TRAJECTORY INTEGRATION

In our previous calculations, the potentials in the lens were calculated using overrelaxation on a 297×41 mesh network covering one-fourth of the lens and assuming a linear behavior of the potentials, not at the gap, but far up in the gap, thus obtaining higher precision for the potentials in the gap. Overrelaxation was continued until a precision of 1 in 10^5 was reached for all points in the network.

Electron trajectories were then calculated and were used in various ways to calculate focal properties[2] and aberrations[13,14] up to the fifth order. The range of voltage ratios covered was from 1.5 to 50. Above these values it was felt that further investigation of the accuracy of the method used was necessary.

Numerical Problems

In Fig. 2 is plotted, for the 1:20 lens (i.e., $V_1/V_2=\frac{1}{20}$), the behavior of the asymptotic axis intersection F_2^* for trajectories entering the lens parallel to the axis at increasing radial distances T. The scale for F_2^* is expanded to show the anomalous behavior of the trajectories entering the lens at $0<T<0.02$ D with respect to those entering at higher T, where D is the diameter of the lens.

The value of F_2^* at which the curve intersects the axis corresponds to F_2 (see Ref. 2). The deviation of this value from an extrapolation of the curve above $T=0.02$ D is of the order of 0.0005 D, which corresponds to the 0.1% error quoted for the focal properties determined with this method.

In order to determine the origin of this effect, the density of the relaxed network was increased, going to a matrix of 593×81. The result was that the effect was enhanced, while points above $T=0.02$ D coincided with those obtained with the first matrix within 1 in 10^4.

Our attention was then drawn to the five-point Lagrange interpolation used to determine potentials within the mesh as the trajectory is calculated. It could be, in fact, that interpolation in general might not be so good in approximating the behavior of the potentials close to the axis as it does off axis. As an alternative method, we chose a least squares fit of a third-order polynomial through the same five points to which Lagrange interpolation was applied.

In Fig. 2 is also shown the result of the best-fit calculated trajectories. Figure 2 refers to the 297×41 matrix, but the result is similar in the denser matrix. Again, we find that points above $T=0.02$ D agree to within 1 in 10^4 with those obtained by interpolation. Below $T=0.02$ D the agreement with the above part of the curve is also better and quite close to what would be predicted by a third-order extrapolation of the curve above $T=0.02$ D to the axis. Incidentally,

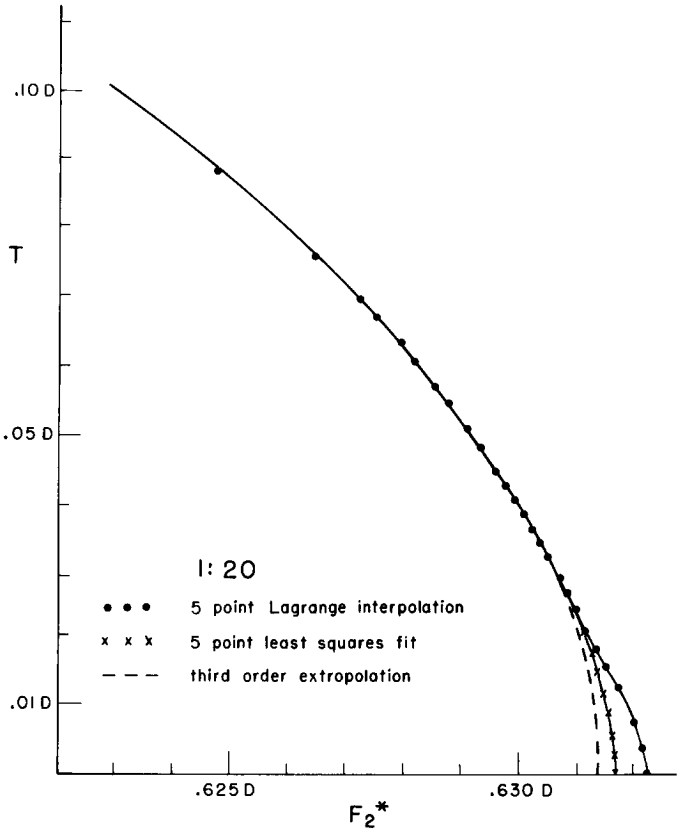

FIG. 2. Plot of the apparent focal point F_2^* for the 1:20 lens as a function of T. (See Fig. 1.)

the curve above $T=0.02$ D agrees with a third-order polynomial, as it should by third-order aberration theory.

The above tests were repeated for several lenses; in all cases the results indicate that the off-axis rays give results compatible to 1 in 10^4, no matter whether interpolation or best fit is used to calculate potentials within the mesh.

Comparison of the behavior of paraxial rays to rays further from the axis seems, therefore, to be a good criterion to determine the accuracy of the calculated focal properties even at higher voltage ratios.

Focal properties for strong lenses up to 1:10 000 were calculated and checked according to the above criterion. It

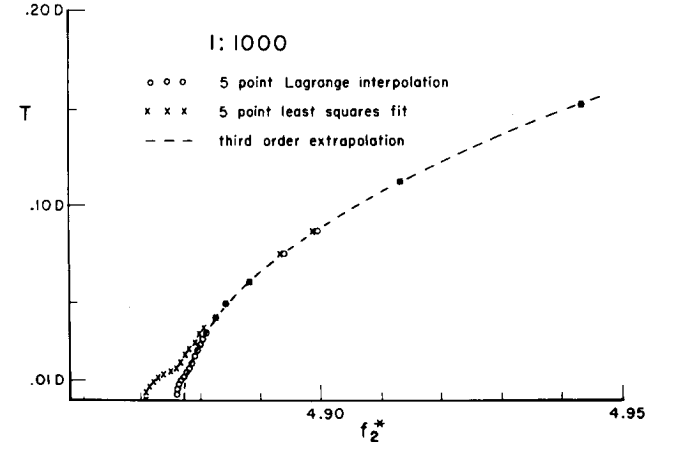

FIG. 3. Plot of the apparent focal length f_2^* for the 1:1000 lens as a function of T. (See Fig. 1.)

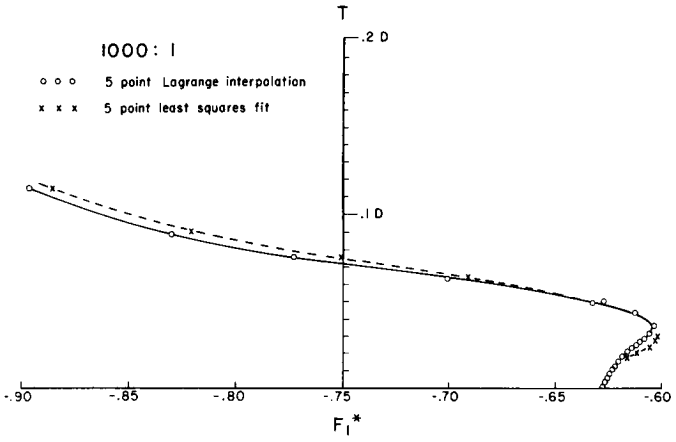

FIG. 4. Plot of the apparent focal point F_1^* for the 1:1000 lens as a function of T'. (See Fig. 1.)

turns out that, as the strength of the lens increases, Lagrange interpolation works better than the best fit method. Figure 3 shows the behavior of the focal length f_2 in the 1:1000 lens and Fig. 4 shows the behavior of F_1. For this reason the focal properties for all the strong lenses were obtained using Lagrange interpolation.

We would like to point out that our focal properties are calculated as the intersection with the axis of the trajectory as specified by its final position and slope. The relative error in this intersection is thus equal to the sum of the relative errors in the final position and slope. Since $|f_1/f_2| = (V_1/V_2)^{\frac{1}{2}}$ is satisfied to a relative accuracy of about 10^{-5}, this implies that the relative accuracy of the position and slope is better than 10^{-5}. Since the final position and slope of typical trajectories used to determine focal properties were of the order of 10^{-3} D and 10^{-3} rad, respectively, the precision of the position and slope must then be of the order of 10^{-8} D and 10^{-8} rad, respectively. Thus trajectories are traced to extremely high precision.

Having established that trajectories are traced to high precision, there remains the question of the absolute accuracy of these trajectories. An examination of Figs. 2 and 3 shows differences up to about 0.1% in the focal properties depending on whether one uses Lagrange interpolation or least squares fitting to interpolate the potentials or use third-order extrapolation of the apparent focal properties.

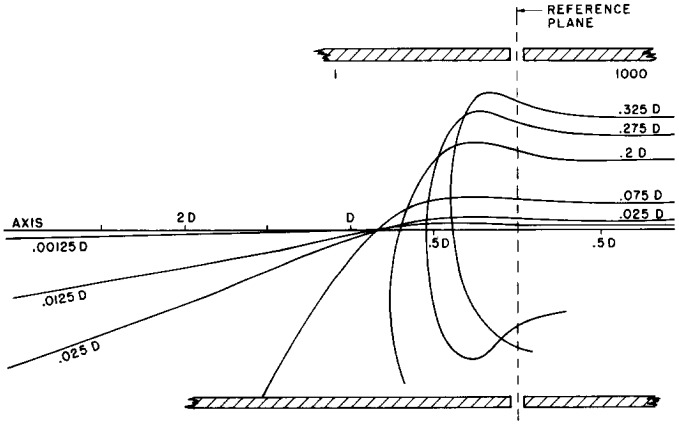

FIG. 5. Plot of various trajectories entering parallel to the axis from the high voltage side of the 1:1000 lens.

Within any one method the precision is clearly better than one part in 10^4. These results imply that the interpolated potentials near the axis are slightly inconsistent with the interpolated potentials farther from the axis. Since both methods of interpolation agree to high precision away from the axis this suggests that polynomial interpolation may be slightly inaccurate near the axis, and also suggests that calculations using only the axial potentials may be subject to a similar error, namely about 0.1%. The interpolation of potentials near the axis merits further investigation.

Since it was found for the 1:1000 lens that for large R, trajectories entering from the higher voltage side are reflected by the fields (see Fig. 5), it was suspected that such an effect would perhaps be due to small accumulated errors in the trajectory calculation. To check this point, the total electron energy (potential+kinetic) was calculated at every point and found equal to its initial energy within 1 in 10^6. In addition the change in potential energy ΔU plus the change in the component of the kinetic energy along the z axis ΔT_z must be equal to the work along R and similarly for z. In other words

$$\int F_R dR = -\Delta U - \Delta T_z, \tag{3}$$

where F_R is the radial component of the force. This relationship was checked over a complete trajectory and found to be valid to better than 1 in 10^6. Here U was determined from interpolation of potentials and F_R obtained from the trajectory program. Therefore, the returning trajectories are real.

RESULTS FOR LARGE VOLTAGE RATIOS

Focal properties of lenses with voltage ratios of 20 to 10 000 were calculated using Lagrange interpolation to determine potentials within each mesh. As before[2,3] trajectories of incident parallel rays were computed and apparent focal points and principal plane positions were calculated from the *final* positions and slopes of the rays for several values of T and T' (see Fig. 1). The true focal points and principal plane positions were then taken to be the limit of the apparent values as the parallel rays approached the axis (T, $T' \to 0$). The results are given in the lower part of Table I. Lenses with voltage ratios near 6400 are close to being telescopic. Therefore, trajectories entering parallel to the axis exit the lens very nearly parallel to the axis, and although these trajectories are traced with high accuracy they do not give a high accuracy for the focal properties. For these lenses it was found that accurate focal properties could be obtained from trajectories which enter the lens so that if undeflected they would pass through the intersection of the axis with the reference plane.

In Table II are given for the stronger lenses the values of $|f_1/f_2|$ and $(V_1/V_2)^{\frac{1}{2}}$ which, in first-order electron optics, should be rigorously equal for rays which enter and leave from field-free regions. This relationship is satisfied to better than 0.003% for all lenses calculated.

In the last column of Table I are given values for $F_1F_2 - f_1f_2$, a quantity which is important when the lens proper-

TABLE I. First-order focal properties of the two-tube electrostatic lens.

V_2/V_1	F_1/D	F_2/D	H_1/D	H_2/D	f_1/D	f_2/D	$F_1F_2-f_1f_2$
1.1	−678.88	678.88	−15.979	−16.364	−662.90	695.24	0.047442
1.2	−185.70	185.68	−8.2834	−8.6695	−177.42	194.35	0.047203
1.3	−89.816	89.777	−5.7201	−6.1070	−84.096	95.884	0.047549
1.4	−54.718	54.663	−4.4395	−4.8276	−50.279	59.490	0.048063
1.5	−37.771	37.701	−3.6720	−4.0613	−34.099	41.763	0.048676
1.7	−22.180	22.085	−2.7962	−3.1884	−19.384	25.274	0.050111
2	−13.133	13.006	−2.1412	−2.5384	−10.992	15.544	0.052573
2.5	−7.6657	7.4958	−1.6343	−2.0406	−6.0313	9.5364	0.057052
5	−2.7683	2.4659	−1.0109	−1.4637	−1.7573	3.9296	0.079318
10	−1.6146	1.1800	−0.81530	−1.3477	−0.79931	2.5276	0.11519
20	−1.1994	0.6322	−0.74466	−1.4017	−0.45479	2.0339	0.16670
40	−1.0210	0.32085	−0.72223	−1.5690	−0.29880	1.8898	0.23711
100	−0.91711	0.041104	−0.71547	−1.9752	−0.20163	2.0163	0.36885
250	−0.85308	−0.19750	−0.69403	−2.7121	−0.15904	2.5146	0.56841
500	−0.78153	−0.39835	−0.63374	−3.7030	−0.14779	3.3046	0.79972
1000	−0.62883	−0.67412	−0.47469	−5.5483	−0.15414	4.8741	1.1752
2000	−0.22281	−1.1848	−0.029506	−9.8297	−0.19331	8.6448	1.9351
3000	0.41935	−1.8592	0.68090	−16.185	−0.26155	14.326	2.9672
4000	1.5934	−3.0045	1.9813	−27.539	−0.38793	24.535	4.7305
5000	4.4392	−5.6891	5.1338	−54.809	−0.69467	49.120	8.8674
6000	21.458	−21.522	23.986	−217.35	−2.5281	195.83	33.260
6200	45.147	−43.517	50.227	−443.49	−5.0798	399.98	67.144
6400	7290.5	−6768.8	8076.0	−69606.	−785.49	62838.	10423.
6600	−50.544	45.293	−55.771	469.94	5.2271	−424.64	−69.668
7000	−18.369	15.417	−20.131	162.78	1.7614	−147.36	−23.642
8000	−8.3706	6.1103	−9.0546	67.288	0.68400	−61.178	−9.3012
9000	−6.0663	3.9486	−6.5017	45.255	0.43542	−41.306	−5.9679
10 000	−5.0422	2.9776	−5.3669	35.450	0.32473	−32.473	−4.4686

ties are represented in matrix form.[8,10,15] We have also included in Table I some of our previous results[2] to present a reasonably complete set of values and also to correct minor misprints in f_2 for the lenses with V_2/V_1 equal to 2 and 2.5. Those readers desiring finer coverage of the voltage ratios between 1.5 and 50 should consult the earlier papers,[1,2] where they will also find comparisons with other values available in the literature for this same range. To our knowledge there are no published results for the two-tube lens at voltage ratios greater than 50.

In Fig. 6(a) trajectories are plotted for the 6400:1 lens to illustrate its near-telescopic property. Note that in the decelerating mode of this lens the telescopic property holds only for rays less than about 0.01 D from the axis. Figures 6(b), (c), (d) show trajectories for the 10 000:1 lens. Figure 6(b) shows parallel rays entering the accelerating lens while Figs. 6(c) and (d) show parallel rays entering the decelerating lens. Note that for the decelerating lens the first-order properties are valid only for parallel rays to about 0.001 D from the axis, and that rays farther from the axis exhibit very irregular behavior, with rays 1, 1.5, and 3 leaving the lens, rays 2 and 6 striking the lower part of the lens and rays 4 and 5 striking the upper part of the lens. Strongly decelerating lenses must be used with great care.

In Fig. 7 we have plotted the focal properties using an arc tangent scaling[16] to compress the wide range of values. The discontinuity of all of the focal properties at $V_2/V_1=1$ and near $V_2/V_1=6400$ and $1/6400$ are clearly evident.

P–Q CURVES

Since it is convenient, when designing electron lens systems, to have the lens data in the form of the P–Q (object–image) curves introduced by Spangenberg and Field[11,12] we give in Figs. 8 and 9 the P–Q curves for voltage ratios from 2 to 10 000. The relevant equations are

$$(P-F_1)(Q-F_2)=f_1f_2, \tag{4}$$

$$M=-f_1/(P-F_1)=-(Q-F_2)/f_2, \tag{5}$$

where M is the magnification. In order to present data over a wide range while giving linearity and continuity near $P=0$ and $Q=0$, an arc tangent scaling of P and Q is used.[9] Since it is common to have virtual objects and images in systems of several lenses, the P–Q curves are given for both real and virtual objects and images. Any object or image inside the lens field (within about 2 D of the lens center) should be considered as virtual. Also included are curves of constant magnification. Those readers desiring a better presentation of P–Q curves for low voltage ratios should consult the earlier papers.[1,2]

Note that for voltage ratios from 2000 to 10 000 an object placed at $P/D=-1.5$ generates a virtual image which is

TABLE II. Test of $|f_2/f_1|=(V_2/V_1)^{\frac{1}{2}}$.

V_2/V_1	$(V_2/V_1)^{\frac{1}{2}}$	$\lvert f_2/f_1\rvert$	Relative difference
100	10.0000	9.99970	3.0×10^{-5}
250	15.8114	15.8110	2.6×10^{-5}
500	22.3607	22.3603	1.7×10^{-5}
1000	31.6228	31.6223	1.6×10^{-5}
2000	44.7214	44.7222	2.0×10^{-5}
3000	54.7723	54.7713	1.7×10^{-5}
4000	63.2456	63.2447	1.4×10^{-5}
5000	70.7107	70.7098	1.3×10^{-5}
6000	77.4597	77.4585	1.5×10^{-5}
6200	78.7401	78.7388	1.7×10^{-5}
6400	80.0000	79.9982	2.3×10^{-5}
6600	81.2404	81.2391	1.6×10^{-5}
7000	83.6660	83.6642	2.2×10^{-5}
8000	89.4427	89.4407	2.3×10^{-5}
9000	94.8683	94.8663	2.1×10^{-5}
10 000	100.0000	99.9982	1.8×10^{-5}

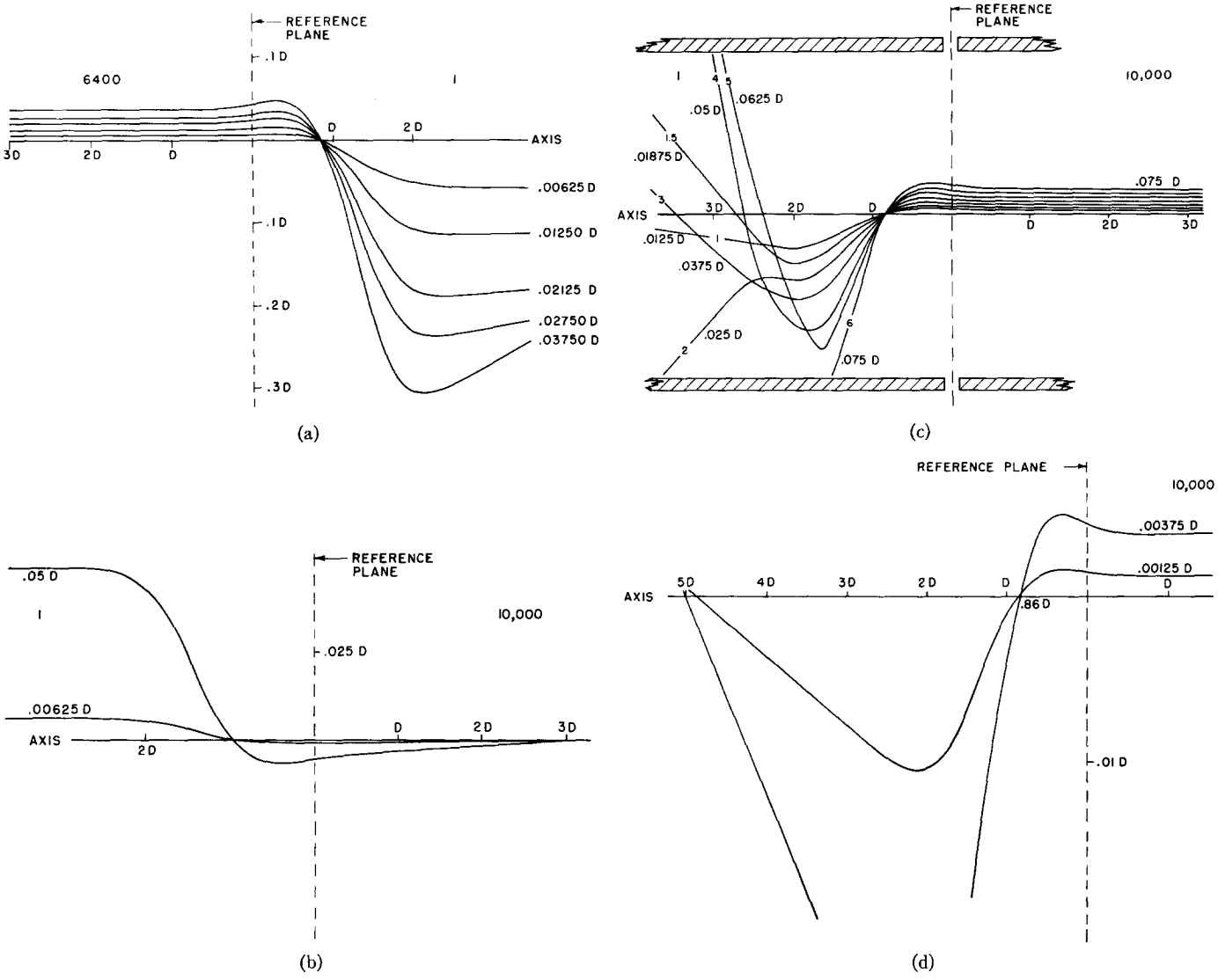

FIG. 6. Plot of various trajectories in very strong lenses. (a) 6400:1 lens; (b), (c), (d) 1:10 000 lens.

close to the reference plane and nearly independent of voltage ratio. A similar effect occurs for voltage ratios from 2 to 40 and $P/D=-0.4$.

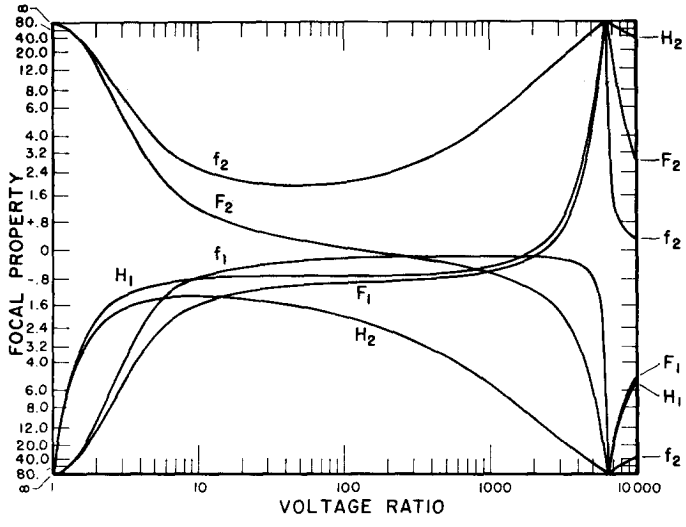

FIG. 7. Plot of the focal properties of the two-tube electrostatic lens.

RESULTS FOR NEAR-UNITY VOLTAGE RATIOS

Focal properties of lenses with voltage ratios between 1.1 and 1.7 were calculated and are given in the upper part of Table I. Note that the quantity $F_1F_2-f_1f_2$ is small and almost constant for weak lenses, even though the quantities F_1, F_2, f_1, f_2 are all rapidly increasing as V_2/V_1 goes to unity.

It was found that all of the data for weak lenses can be well-represented as simple functions of the parameter $\gamma=(V_2/V_1)^{\frac{1}{2}}$ which was previously used by Grivet[17] in formulas for the two-tube lens. The equations are

$$-F_1=F_2=0.38546[\gamma/(\gamma-1)^2], \quad (6)$$

$$f_1=-0.38546[1/(\gamma-1)]^2, \quad (7)$$

$$f_2=0.38546[\gamma/(\gamma-1)]^2, \quad (8)$$

$$H_1=-0.38546[1/(\gamma-1)], \quad (9)$$

$$H_2=-0.38546[\gamma/(\gamma-1)]. \quad (10)$$

Table III shows the results of a test of Eqs. (6)–(8), performed by dividing the true values of f_1, f_2, F_1, F_2 by the values from Eqs. (6)–(8). As can be seen the approximation

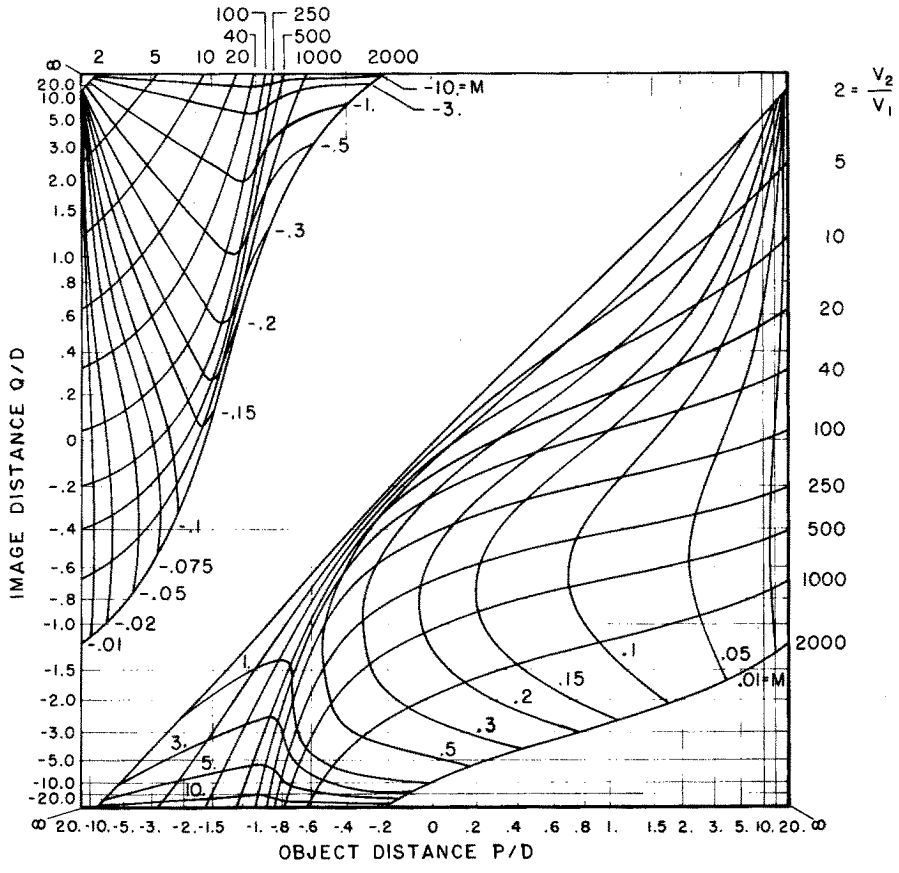

FIG. 8. *P–Q* curves for the two-tube electrostatic lens for voltage ratios from 2 to 2000. *P* is the object distance measured from the reference plane (see Fig. 1), and is negative to the left. *Q* is the image distance measured from the reference plane and is positive to the right.

is very good, with deviations less than 0.7% at a voltage ratio of 1.5, and deviations only slightly larger than 2% at a voltage ratio of 2.

Read *et al.*[1] recommended that interpolation between given values of V_2/V_1 can best be accomplished, at values of V_2/V_1 which are near unity, by using the parameters

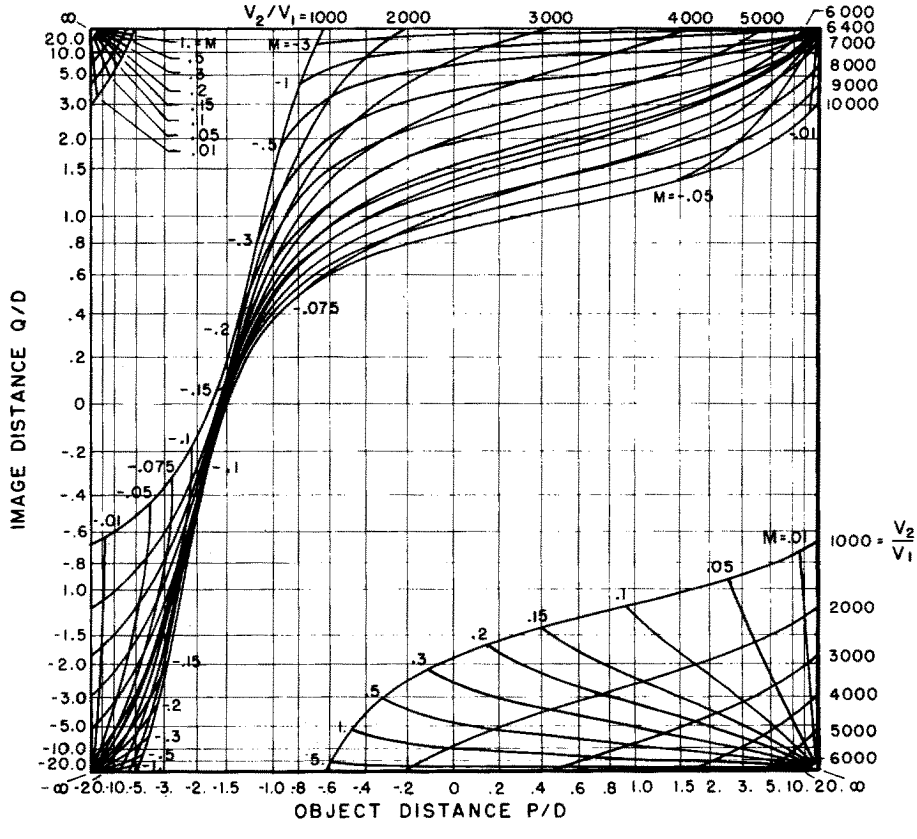

FIG. 9. *P–Q* curves for the two-tube electrostatic lens for voltage ratios from 1000 to 10 000.

TABLE III. Test of Eqs. (6)–(8) for weak lenses.

$\frac{V_2}{V_1}$	$-f_1(\gamma-1)^2$	$f_2\left(\frac{\gamma-1}{\gamma}\right)^2$	$-F_1\left(\frac{\gamma-1}{\gamma}\right)^2$	$F_2\left(\frac{\gamma-1}{\gamma}\right)^2$
1.1	0.38546	0.38546	0.38545	0.38545
1.2	0.38585	0.38585	0.38588	0.38584
1.3	0.38646	0.38646	0.38655	0.38637
1.4	0.38721	0.38721	0.38741	0.38701
1.5	0.38808	0.38808	0.38844	0.38772
2	0.39349	0.39349	0.39535	0.39153

$f[(V_2/V_1)-1]^2$ which they claimed are approximately constant for weak lenses. The test of this relation is given in Table IV. As can be seen, this is a poor approximation, with deviations up to about 25% between voltage ratios of 1.1 and 1.3, a range where Eqs. (6)–(8) show deviations of approximately a factor of a hundred less.

DISCUSSION

Accurate values of first-order focal properties are now available for the two-tube electrostatic lens over a wide range encompassing both very weak and very strong lenses. Confidence in the accuracy of the data is enhanced by the excellent agreement (about 0.1%) between our results and those of Read *et al.*[1] for voltage ratios of 1.5 to 50. The usefulness of the data is increased by the presentation of P–Q curves and by the existence of an accurate approximation to the focal properties of very weak lenses.

TABLE IV. Test of equation from Ref. 1 for weak lenses.

$\frac{V_2}{V_1}$	$-f_1\left(\frac{V_2}{V_1}-1\right)^2$	$f_2\left(\frac{V_2}{V_1}-1\right)^2$	$-F_1\left(\frac{V_2}{V_1}-1\right)^2$	$F_2\left(\frac{V_2}{V_1}-1\right)^2$
1.1	6.629	6.952	6.789	6.789
1.2	7.097	7.774	7.428	7.427
1.3	7.569	8.630	8.083	8.080

ACKNOWLEDGMENT

One of us (CEK) thanks Dr. Read for showing him some of his results for strong lenses prior to publication.

*Work supported by the Consiglio Nazionale delle Ricerche, Italy.

[1]F. H. Read, A. Adams, and J. R. Soto-Montiel, J. Phys. E **4**, 625 (1971).
[2]S. Natali, D. DiChio, E. Uva, and C. E. Kuyatt, Rev. Sci. Instrum. **43**, 80 (1972).
[3]S. Natali, D. DiChio, and C. E. Kuyatt, J. Res. Natl. Bur. Stand. A **76**, 27 (1972).
[4]F. H. Read, private communication.
[5]J. D. Cross, F. H. Read, and E. A. Riddle, J. Sci. Instrum. **44**, 993 (1967); R. E. Imhof and F. H. Read, J. Phys. E **1**, 859 (1968); F. H. Read, J. Phys. E **3**, 127 (1970); A. Adams and F. H. Read, J. Phys. E **5**, 156 (1972).
[6]D. W. O. Heddle, J. Sci. Instrum. **2**, 1046 (1969).
[7]C. E. Kuyatt and E. W. Plummer, Rev. Sci. Instrum. **43**, 108 (1972).
[8]A. Galejs and C. E. Kuyatt, J. Vac. Sci. Technol, **10**, 1114 (1973).
[9]C. E. Kuyatt, D. DiChio, and S. V. Natali, J. Vac. Sci. Technol. **10**, 1118 (1973).
[10]C. E. Kuyatt, "Electron Optics Notes," lectures delivered at NBS, April, May, 1967 (unpublished).
[11]K. R. Spangenberg and L. M. Field, Elec. Commun. **21**, 194 (1943).
[12]K. R. Spangenberg, *Vacuum Tubes* (McGraw-Hill, New York, 1948).
[13]C. E. Kuyatt, S. V. Natali, and D. DiChio, *Record of 11th Symposium on Electron, Ion, and Laser Beam Technology*, edited by R. F. M. Thornley (San Francisco Press, Inc., San Francisco, 1971).
[14]C. E. Kuyatt, S. V. Natali, and D. DiChio, Rev. Sci. Instrum. **43**, 84 (1972).
[15]C. E. Kuyatt, S. V. Natali, and D. DiChio, Rev. Sci. Instrum. **45**, 566 (1974).
[16]W. Glaser, *Grundlagen der Elektronenoptik* (Springer, Vienna, 1952), p. 133, has also used the arc tangent scaling to represent quantities which become infinite at some point of their range.
[17]P. Grivet, *Electron Optics* (Pergamon, Oxford, 1965), p. 164 ff.